AD-A034 681 NOTRE DAME UNIV IND DEPT OF METALLURGICAL ENGINEERI--ETC F/G 20/2
MAGNETIZATION, MAGNETOCRYSTALLINE ANISOTROPY AND MAGNETOSTRICTI--ETC(U)
DEC 76 A E MILLER, C W ALLEN, T D'SILVA N00014-75-C-0977
UNCLASSIFIED TR-12/76 NL

| OF |
AD
A034681

END

DATE
FILMED
2-77

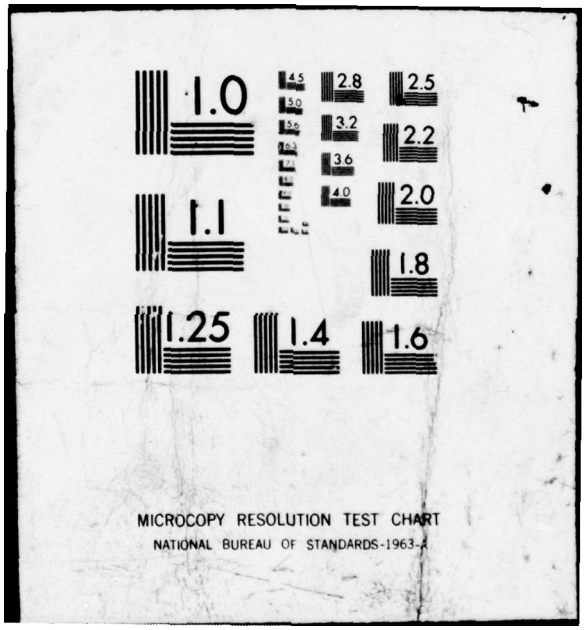
1.0
1.1
1.25
1.4
1.6
1.8
2.0
2.2
2.5
2.8
3.2
3.6
4.0
4.5
5.0
MICROCOPY RESOLUTION TEST CHART
NATIONAL BUREAU OF STANDARDS-1963-A

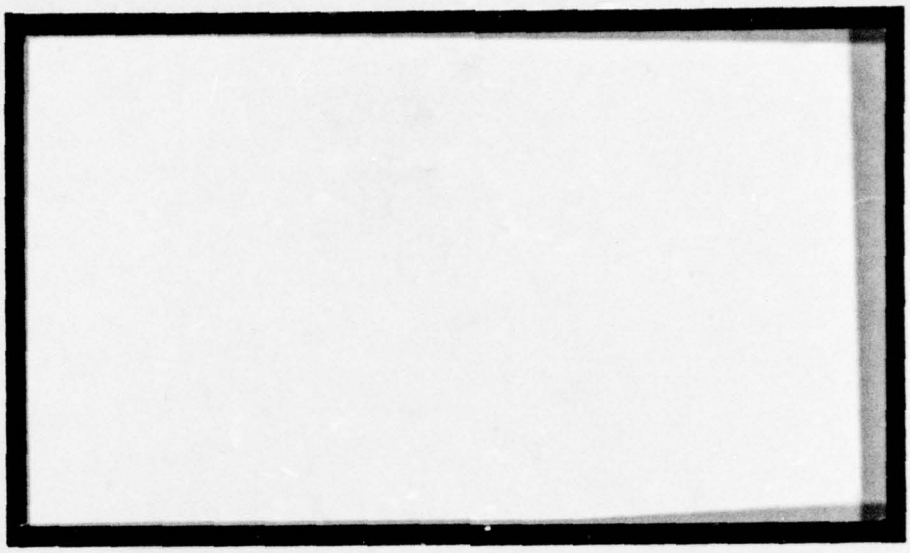

University of Notre Dame
Department of
Metallurgical Engineering
and Materials Science
Notre Dame, Indiana
46556

(6)

MAGNETIZATION, MAGNETOCRYSTALLINE ANISOTROPY AND MAGNETOSTRICTION IN SOME RARE-EARTH-COBALT COMPOUNDS, R_2Co_{17}.

(10) A. E. Miller, C. W. Allen, T. D'Silva, H. Rodrigues K. C. Liao

(11) December 1976

(12) 16p.

Department of Metallurgical Engineering
and Materials Science
University of Notre Dame
Notre Dame, Indiana 46556

(15) Contract N00014-75-C-0977 NEW
Office of Naval Research

(9) TECHNICAL REPORT, NO.
(14) MTR-12/76

400656

4B

FOREWORD

This technical report was prepared by the Magnetic Materials Properties Group at the University of Notre Dame, Department of Metallurgical Engineering and Materials Science. Of the coauthors, Dr. A. E. Miller and Dr. C. W. Allen are respectively, Associate Professor and Professor of Metallurgical Engineering and Materials Science. Dr. T. D'Silva is a Post Doctoral Associate and H. Rodrigues and K. C. Liao are Graduate Research Assistants.

The research was performed under the sponsorship of the Department of the Navy, Office of Naval Research, Arlington, Virginia 22217, with funding under Contract No. N00014-75-C-0977 Metallurgy Program, Office of Naval Research, Mr. W. G. Rauch, Director.

The authors express their appreciation to Mrs. J. Peiffer for her diligence in preparation of this manuscript.

This technical report has been reviewed and approved for submittal to the sponsoring agency on December 30, 1976.

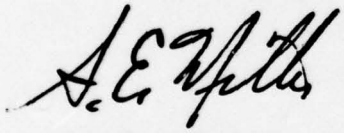

A. E. MILLER
Group Leader
Magnetic Materials
Properties

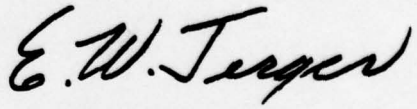

EDWARD W. JERGER
Associate Dean
College of Engineering

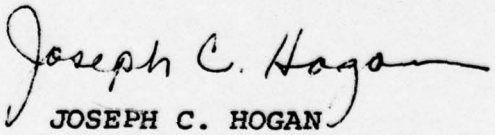

JOSEPH C. HOGAN
Dean, College of Engineering
University of Notre Dame

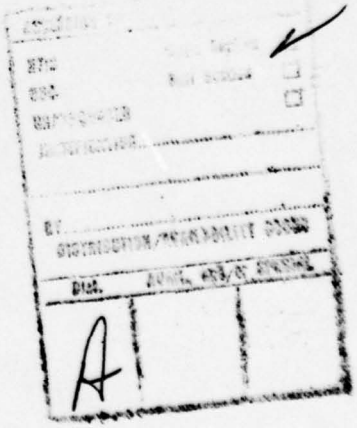

12th RARE EARTH RESEARCH CONFERENCE

July 18-22, 1976
Vail, Colorado

MAGNETIZATION, MAGNETOSTRICTION AND MAGNETOCRYSTALLINE ANISOTROPY IN SOME R_2Co_{17} COMPOUNDS

A. E. Miller* and T. D'Silva

Department of Metallurgical Engineering and Materials Science
University of Notre Dame, Indiana 46556

Introduction: The purpose of this paper is to presents the results of a study of the temperature dependence of the saturation magnetization, magnetocrystalline anisotropy and magnetostriction of the R_2Co_{17} compounds (R=Y, Tb, Dy, Ho, Er, Tm and Lu) and the pseudobinary alloys $Y_{2x}Dy_{2(1-x)}Co_{17}$ and $Lu_{2x}Tm_{2(1-x}Co_{17}$ (where x = 1/3, 2/3).

The magnetocrystalline anisotropy energy[1] in the hexagonal R_2Co_{17} compounds is given by,

$$E_A = K_1\sin^2\theta + K_2\sin^4\theta \qquad (1)$$

where θ is the angle between the magnetization vector M_s and the hexagonal C-axis. K_1 and K_2 are determined by a least square fit of the measured magnetization curve along the hard axis to the theoretical equations of magnetization given by Sucksmith and Thompson[2]. The magnetically induced strain in the hexagonal compounds as a function of the direction of strain measurement, direction of magnetization and the magnetostriction constants λ^γ, λ^ε and λ^α is given by Callen and Callen[3]. The magnetostriction constant λ^γ describes the distortion in the basal plane[4].

Callen and Shtrickman[5] have shown that the temperature dependence of the spin averages can be represented by a hyperbolic Bessel function of the reduced magnetization. Therefore, if the magnetic behavior of the rare earth ion is single ion in nature, the magnetostriction constant (λ^R) and the anisotropy coefficients (k^R) of the rare earth sublattice, denoted by the superscript R, can be related to the magnetization of the rare earth sublattice by the following relationship.

$$\lambda^R(T,H) = \lambda^R(O,H)\,\hat{I}_{\ell+\frac{1}{2}}\left(\mathcal{L}^{-1}\,\frac{m(T,H)}{m(O,H)}\right) \qquad (2)$$

$$k^R(T,H) = k^R(O,H)\,\hat{I}_{\ell+\frac{1}{2}}\left(\mathcal{L}^{-1}\,\frac{m(T,H)}{m(O,H)}\right) \qquad (3)$$

where,
$$\lambda^R(T,H) = \lambda^{R_2Co_{17}}(T,H) - \lambda^{Co}(T,H) \qquad (4)$$

$$k^R(T,H) = k^{R_2Co_{17}}(T,H) - k^{Co}(T,H) \qquad (5)$$

$$m^R(T,H) = m^{R_2Co_{17}}(T,H) - m^{Co}(T,H) \qquad (6)$$

and $\mathcal{L}^{-1}\,\frac{m(T,H)}{m(O,H)}$ is the inverse Langevin function of the reduced magnetization.

An additional criteria for single ion behavior is the direct dependence of the magnitude of magnetization, anisotropy and magnetostriction of the rare-earth sublattice on the fraction of rare-earth ion in the compound[6].

If $\lambda^R(O,H)$ and $k^R(O,H)$ is known for one type of ion, it is possible to predict the values of these constants for the other rare earth ions from the following relationship[7,8].

$$\frac{\lambda^{R1}(O,H)}{\lambda^{R2}(O,H)} = \frac{k^{R1}(O,H)}{k^{R2}(O,H)} = \frac{\alpha_1 J_1(J_1-\frac{1}{2})\,\langle r_f^2\rangle_1}{\alpha_2 J_2(J_2-\frac{1}{2})\,\langle r_f^2\rangle_2} \qquad (7)$$

where, R_1, R_2 are two types of rare earth ions, α is the Stevens equivalent operator coefficient, and $\langle r_f^2\rangle$ is the average square of the orbital radius of the 4f electron.

Experimental: The saturation magnetization, magnetostriction constant λ^γ and magnetization curves in the easy and hard directions, were determined from 77.4°k to 450°k on single crystals of the R_2Co_{17} compounds and pseudobinaries. Details of specimen preparation and experimental technique have been described in previous papers[9,10,11,12].

Results and Discussion: Y_2Co_{17}, Dy_2Co_{17}, Tb_2Co_{17}, Ho_2Co_{17} and the pseudobinaries in the Y_2Co_{17}-Dy_2Co_{17} system are all easy basal plane, while Tm_2Co_{17}, Er_2Co_{17} and the pseudobinaries in the Tm_2Co_{17}-Lu_2Co_{17} system are easy C-axis in the temperature range 77.4°k to 400°k. The two pseudobinaries in the Y_2Co_{17}-Dy_2Co_{17} system develop basal plane anisotropy at low temperatures. Lu_2Co_{17} is easy basal at 77.4°k and develops an easy cone as a function of increasing temperature. The directions of easy magnetization of all the compounds except Lu_2Co_{17} are in good agreement with that reported in literature[13]. The difference in easy direction between the Lu_2Co_{17} single crystal used in this study and the aligned powders of Lu_2Co_{17} of Givord and Lemaire[14] who used the x-ray intensity technique, may be due to a difference in composition. Such a composition dependence of the direction of easy magnetization has been reported for Y_2Co_{17}[13].

The temperature dependence of the saturation magnetization of all the compounds is shown in Fig. 1. The x-ray densities of the compounds determined by Strnat and Ostertag[16] were used to obtain emu/cc. Yttrium and Lutetium are non-magnetic and therefore the magnetic behavior of Y_2Co_{17} and Lu_2Co_{17} is essentially that of cobalt. The magnetization of the magnetic sub-

lattices of Tb, Dy, Ho, Er and Tm substract from that of the cobalt sublattice according to the ferrimagnetic model for heavy rare earths, as described by Strnat[13].

The room temperature saturation magnetization values agree very well with those reported by Strnat et al[17] for all the compounds except Ho_2Co_{17} and Tb_2Co_{17}. The data obtained by these authors was from aligned powders and the saturation magnetization values were corrected for the presence of cobalt in these samples Secondly, the magnetization values are extrapolated values for most of the compounds. A further comparison of saturation magnetization values at room temperature and 77.4°k with those reported on aligned powders by Laforest et al[16] again shows lack of agreement for Tm_2Co_{17}, Ho_2Co_{17} and Er_2Co_{17}. However Laforest et al indicate that there could be a large error for these compounds because of the likelihood of lack of saturation. The saturation magnetization values reported by Narasimhan and Wallace[19] for Lu_2Co_{17}, Tm_2Co_{17} and Er_2Co_{17} are consistently higher than those reported here which could indicate that their samples are richer in cobalt.

Fig. 2 shows the magnetostriction constant λ^γ for Tb_2Co_{17}, Lu_2Co_{17}, Y_2Co_{17} and Dy_2Co_{17}. λ^γ for Dy_2Co_{17} changes sign at about 100°K.

The temperature dependence of the anisotropy constant K_1 for all the compounds is shown in Fig. 3. K_1 is positive for Er_2Co_{17} and Tm_2Co_{17} which are easy C-axis. The anisotropy of Tb_2Co_{17} and Dy_2Co_{17} is extremely high at low temperatures and therefore the accuracy of determining K_1 is low. The anisotropy constant K_1 for Y_2Co_{17} agrees well with that reported by Strnat[20]. The room temperature values of K_1 for aligned powders of Tm_2Co_{17} and Er_2Co_{17} reported by Narasimhan and Wallace[19] are much lower. ($K_1^{Er_2Co_{17}} = 0.27 \times 10^7$ ergs/cc, $K_1^{Tm_2Co_{17}} = 0.43 \times 10^7$ ergs/cc).

Figs. 4, 5, 6 show the contribution of the Dy sublattice to M_s, λ^γ and K_1. The contribution of the Dy sublattice to M_s, λ^γ and K_1 was obtained from eq. 4, 5, and 6.

Figs. 7 and 8 show the contribution of the Tm sublattice to M_s and K_1 of Tm_2Co_{17} and the two pseudobinaries. The cobalt contribution to K_1 in these compounds was determined from pure cobalt[21] which has an easy axis as in the case of Tm containing compounds.

The contribution of the Dy and Tm sublattices to the R_2Co_{17} compounds are directly proportional to the fraction of rare earth ions in the compound within reasonable limits. The exact compositions of these compounds are as yet undetermined. Also,

in calculating M_s, it has been assumed that the densities are a linear function of composition of the pseudobinaries which may not be true. These two factors could account for the deviations from direct proportionality observed in some of the pseudobinaries.

The dependence of λ^γ and K_1 for the Dy sublattice and K_1 for the Tm sublattice on the rare earth sublattice magnetization are shown in Figs. 9(a,b), and 10 respectively. Differences between behavior in the different compounds in the same system could be due to the crystal field effects resulting from differing c/a ratios for the different rare earth contents. Corrections for this effect have not been made to date. This is similar to the magnetoelastic contribution to anisotropy observed in the pure rare earths[8,22].

The dependence on magnetization of K_1^{Er} and K_1^{Ho}, K_1^{Tb} and $(\lambda^\gamma)^{Tb}$ are shown in Figs. 11, 12 respectively. K_1^{Er} shows good agreement with single ion behavior, whereas K_1^{Ho} and K_1^{Tb} do not. This could be due to the lack of high field, hard-axis magnetization data necessary for accurately determining K_2^{Ho} and K_2^{Tb} which may be significant in these compounds. λ^γ for the Tb ion shows excellent agreement with single ion behavior.

Table I shows a comparison between the $\lambda^\gamma(O,H)$ and $K(O,H)$ determined experimentally and those predicted by equation (7) with dyposium as a basis of comparison. The predictions for $K^\gamma(O,H)$ are in excellent agreement with experiment. The discrepancy for the magnetostriction of the Tb ion is not understood.

Conclusions: The direct dependence of the magnetization, anisotropy and magnetostriction on the rare-earth content indicate that Dy and Tm may be single ion in nature in the R_2Co_{17} compounds. However, the composition, dependence of the crystal field interaction on c/a ratio and the anisotropy constant K_2 has to be determined before the single ion nature of the rare earth ions can be fully documented.

References:

1. W. P. Mason, Phys. Rev., 96, 302, (1954).
2. W. Sucksmith and J. E. Thompson, Proc. Roy. Soc., 225, 362, (1954).
3. E. Callen and H. Callen, Phys. Rev., 139, A455 (1965).
4. A. E. Clark, B. F. Desavage and R. Bozorth, Physical Review, 138, 216, (1965).
5. H. Callen and S. Shtrickman, Solid State Communication, 3, 5, (1965).
6. A. E. Clark, J. J. Rhyne and E. R. Callen, Journal of Appl.

Physics, 39, No. 2, 573 (1968).
7. N. Tsuya, A. E. Clark, R. M. Bozorth, Proceedings of the International Conference on Magnetism, 250 (1964).
8. M. I. Darby and E. D. Isaac, IEEE Transactions on Magnetics, 10, No. 2, (1974).
9. T. D'Silva, H. Igarashi and A. E. Miller, Proceedings of the 10th Rare Earth Research Conference, 1, 458, (1973).
10. A. E. Miller, T. D'Silva, H. Igarashi and J.Shanley, AIP Conference Proceedings, 19th Annual Conference on Magnetism and Magnetic Materials, 2, 1253 (1974).
11. A. E. Miller, T. D'Silva and K. Miura, Proceedings of the Eleventh Rare Earth Research Conference, 1, 461, (1974).
12. A. E. Miller, J. F. Shanley, III and T. D'Silva, Proceedings of the 11th Rare Earth Research Conference, 2, 469, (1974).
13. K. J. Strnat, AIP Conference Proceedings, No. 5, 1047 (1971).
14. F. Givord and R. Lemaire, Solid State Communication, 9, 341, (1971).
15. Masaaki Hamano, Seishi Yajima and Hiromichi Umebayashi, IEEE Transactions on Magnetics, 518, (Sept. 1972).
16. W. Ostertag and K. J. Strnat, Acta Cryst., 21, 560, (1966).
17. K. Strnat, G. Hoffer, W. Ostertag and J. C. Olson, J. Appl. Phys., 37, 1252 (1966).
18. J. Laforest, R. Lemaire, R. Pauthenet and J. Schweiger, C.R. Acad. Sci. Paris, 262, 1260 (1966).
19. K.S.V.L. Narasimhan and W. E. Wallace, AIP Conference Proceedings, No. 18, Part 2, 1212 (1973).
20. G. Hoffer and K. Strnat, Journal of Applied Physics, 18, No. 3, (1967).
21. Y. Barnier, R. Pauthenet and G. Rimet, Cobalt, 15, 1, (1962).
22. B. R. Cooper, Phys. Rev., 169, 281, (1968).

Table I. Comparison of theoretical and experimental coefficients.

	Tb	Dy	Ho	Er	Tm
$\alpha(r^2)(J(J-\frac{1}{2})$	104	100	38	-37	-88
$\lambda^Y(0)$ expt.	+123	-232			
$\lambda^Y(0)$ theoretical	-241	-232	-89	88	204
$K_1(0)\times 10^7$ expt.	-25	-31.6	-13.5	+10.3	43
$K_1(0)\times 10^7$ theoretical	-33	-31.6	-12.0	+11.7	+28

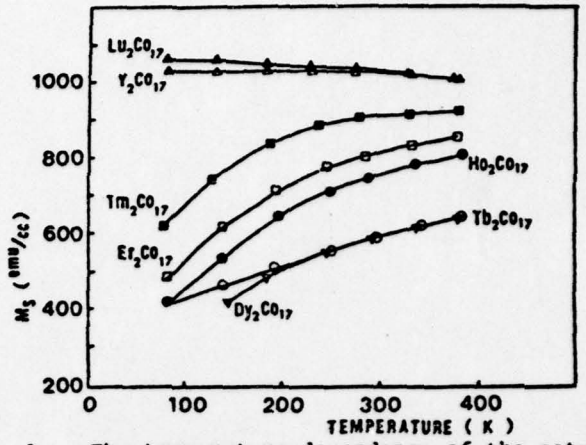

Fig. 1. The temperature dependence of the saturation magnetization (M_s) for the R_2Co_{17} compounds.

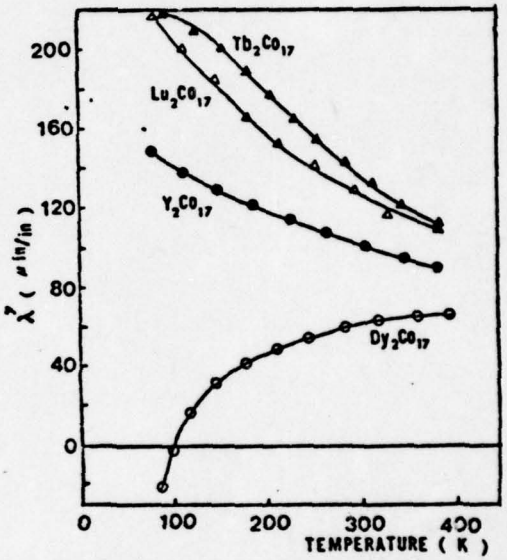

Fig. 2. The temperature dependence of the magnetostriction constant λ^Y.

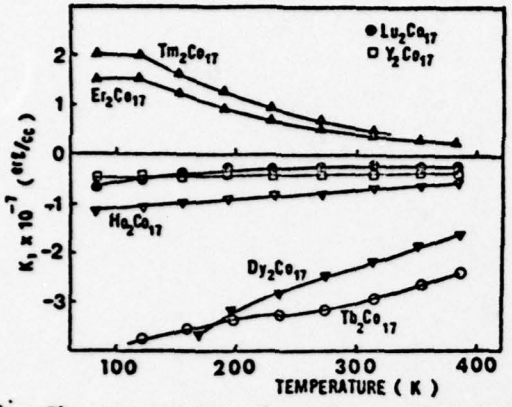

Fig. 3. The temperature dependence of the anisotropy constant K_1 for the R_2Co_{17} compounds.

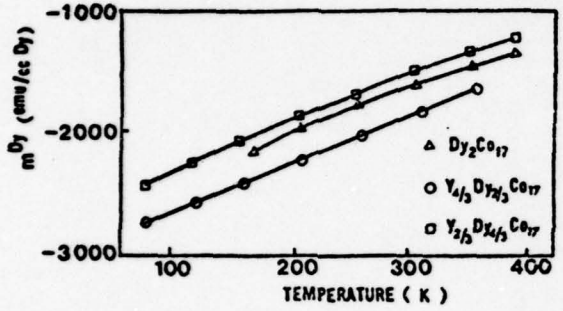

Fig. 4. The Dy sublattice contribution to the saturation magnetization.

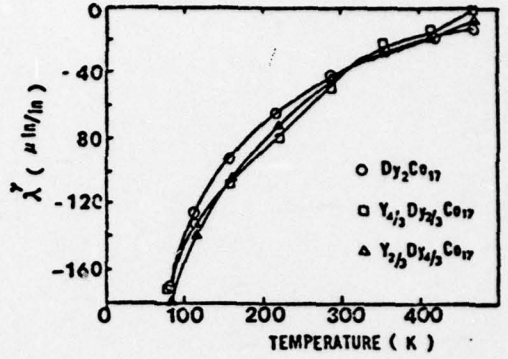

Fig. 5. The Dy sublattice contribution to magnetostriction

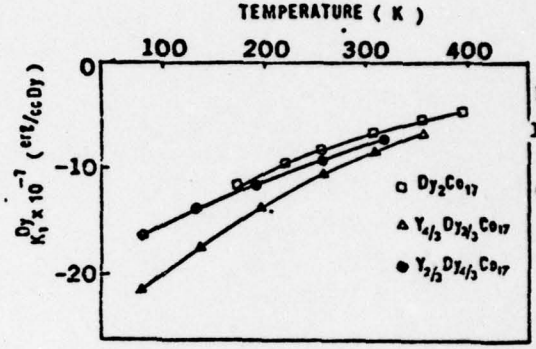

Fig. 6. The Dy sublattice contribution to the anisotropy constant K_1.

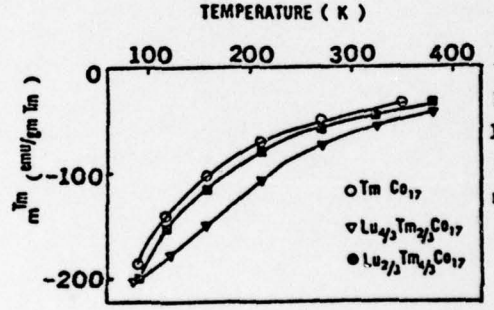

Fig. 7. The Tm sublattice contribution to the saturation magnetization.

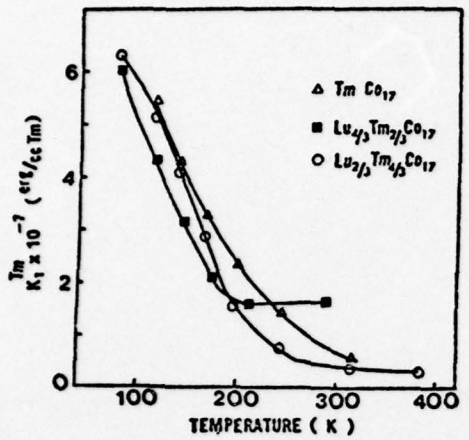

Fig. 8. The Tm sublattice contribution to the anisotropy constant K_1.

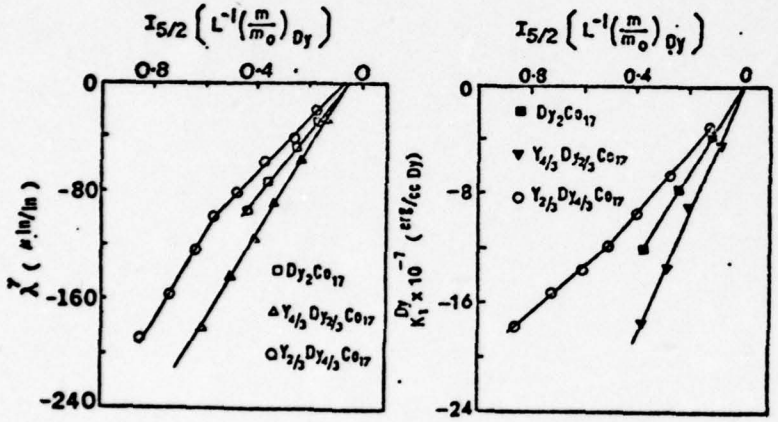

Fig. 9. The dependence on magnetization of the Dy sublattice contribution to (a) λ^Y (b) K_1.

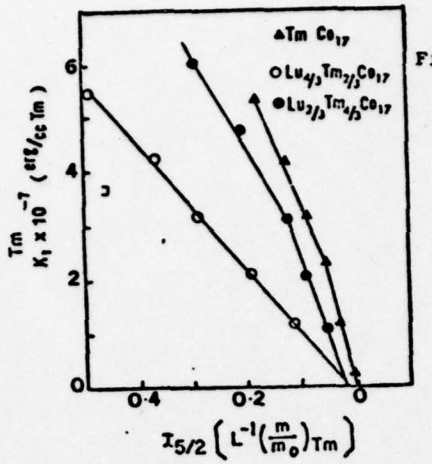

Fig. 10. The dependence on magnetization of the Tm sublattice

Fig. 11. The dependence on magnetization of K_1^{Er} and K_1^{Ho}.

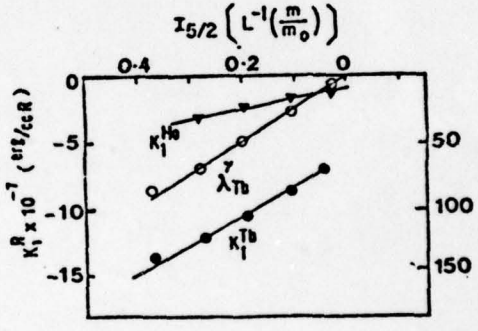

Fig. 12. The dependence on magnetization of $(\lambda^Y)^{Tb}$ and $(K_1)^{Tb}$.

12th RARE EARTH RESEARCH CONFERENCE

July 18-22, 1976

Vail, Colorado

Fault Structures in Rare Earth-Cobalt Intermetallics

C. W. Allen, K. C. Liao and A. E. Miller*

Department of Metallurgical Engineering
and Materials Science
University of Notre Dame
Notre Dame, IN 46556

Introduction: In dealing with materials which may undergo a shear (simple martensitic) transformation or which may contain planar compositional faulting, it is valuable to employ a stacking sequence notation, a structural symbolism, which may be developed for any layer-like structure. The purpose of this paper is to present such a conventional notation, as far as possible consistent for all possible phases in rare earth-transition element systems ranging from RCo_2 through R_2Co_{17}, and then to illustrate briefly application of this notation to shear transformations, shear structure development and the nature of homologous series of phases within such systems.

Ideal Structures: The various structures exhibited by R-Co analogs of phases such as AB_2, AB_3, A_2B_7, AB_5 and A_2B_{17} have been well documented and shown to be closely related to one another (1,2,3,4). This is illustrated in Fig. 1 for the 2H form of AB_2, AB_3 and A_2B_7 and for AB_5 for which only 1H is possible. In the frist three cases rhombohedral forms (3R) are also well known. In this form the Laves phase AB_2 is usually face-centered cubic or nearly so.

It is clear from Fig. 1 that stacking sequence models of these structures may be made which contain four ingredient layers, demonstrated for AB_2 and AB_5 in Figs. 2 and 3. These show exploded views of the layers which make up the fundamental stacking units of the respective structures. With reference to the R-Co phases, the layer elements are

1. A loosely packed R-layer in RCo_2 (to be designated α, β, or γ). 1 R-atom per unit cell layer.
2. A nearly close packed Co-layer with ordered omissions in RCo_2 and RCo_5 ($(Co)_A$, $(Co)_B$ or $(Co)_C$). 3 Co-atoms per unit cell layer.
3. A dispersed Co-layer in RCo_2 (a, b or c). 1 Co-atom per unit cell layer.
4. A topologically close packed mixed layer containing 2 Co to 1 R in RCo_2 (x, y or z). 2 Co-atoms and 1 R-atom per unit cell layer.

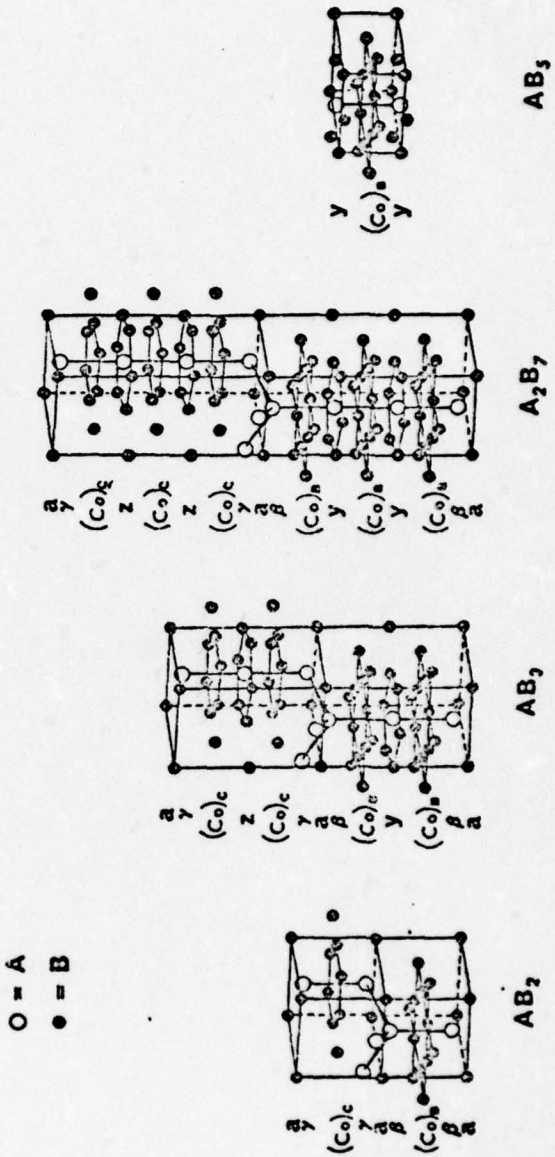

Fig. 1. Unit cells for the 2H modifications of RCo_2, RCo_3 and R_2Co_7 and for the 1H RCo_5 (after Ref. 1 and 2). Stacking sequence representation is included for each.

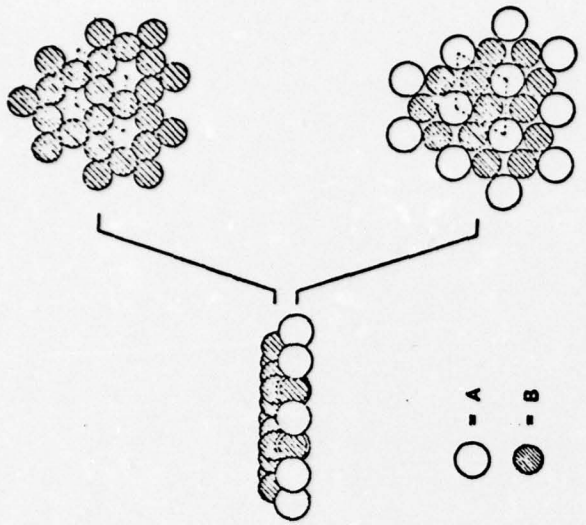

Fig. 3. Basic layer unit of $CaCu_5$ structure.

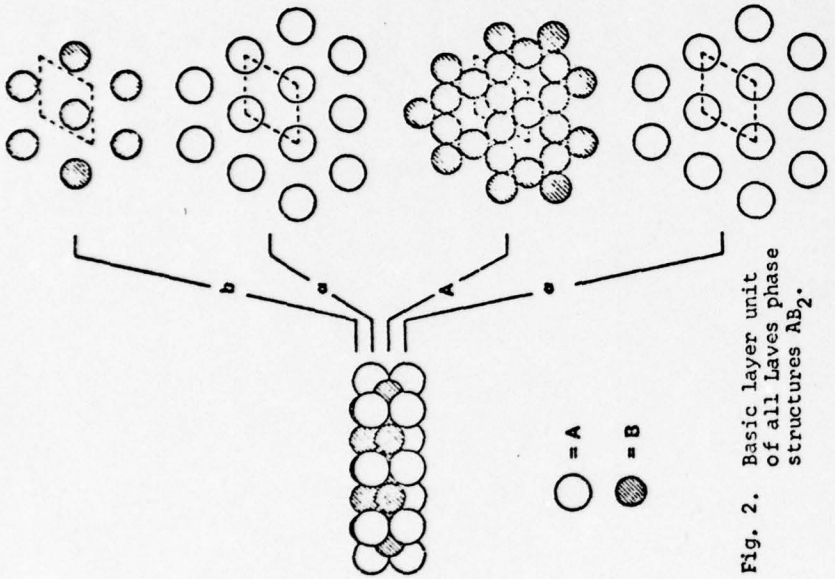

Fig. 2. Basic layer unit of all Laves phase structures AB_2.

Various combinations of these layers result in an endless sequence of compositions between RCo_2 and RCo_5, which include those proposed by Strnat and Ray (4). RCo_3 and R_2Co_7 are two such possibilities.

The Greek and Roman symbols provide a shorthand representation of the position of a given layer with respect to some fixed reference grid, just as the designation ...ABABCBCAC... does for the Sm structure. The reference grid is shown in Fig. 4 in terms of "key positions" X, Y and Z. The subscripts 1,2,3 are superfluous except for subsequent discussion of R_2Co_{17}. Conventions for naming the layer positions are summarized in Table 1. Except for the compact Co-layers ($(Co)_A$, $(Co)_B$, $(Co)_C$), the position designations are determined by obvious atom positions (in the mixed layer, the R-positions, except in R_2Co_{17}). For compact Co-layers, the designation follows the positions of atom omission. The stacking sequences resulting from these conventions are included in Fig. 1.

For the phases R_2Co_{17}, the mixed R-Co layer (Fig. 3) is modified as shown in Fig. 5, with 1/3 of the R-atoms replaced by Co-pairs ordered, as shown, in the hexagonal and rhombohedral forms of these phases. As a consequence the base section of each unit cell is larger than that for the other R-Co phases. For R_2Co_{17}, $\bar{a}_1$ and $\bar{a}_2$ are indicated in Fig. 5 in relation to those for the other phases. Now the subscripted key position designations of Fig. 4 are necessary as summarized in Table 1, with position of the mixed layer keyed to the positions of the Co-pairs, not of the R-atoms.

Thus an ordered 2H form of R_2Co_{17} is represented

$$...x_1(Co)x_2(Co)x_1(Co)...$$

and a 3R form,

$$... x_1(Co)x_2(Co)x_3(Co)x_1(Co)...$$

as has been discussed previously with a slightly different stacking sequence notation (5,6).

Transformations and Faults: Diffusionless shear transformations of the type 2H ⇌ 3R have been demonstrated for virtually all R-Co phase types except RCo_5 in which this is not possible structurally.

Shear transformations result from structural faulting accompanying the glide of Shockley-type partial dislocations which, under the circumstances, may be called glissile transformation dislocations. With respect to the initial structure, such glide

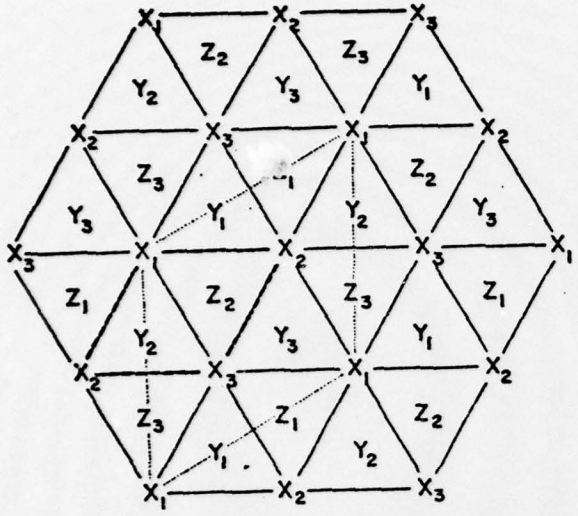

Fig. 4. Key layer positions for the rare earth-cobalt phases RCo_2 through R_2Co_{17}. Numerical subscripts refer only to R_2Co_{17}. Unit cells for RCo_2-RCo_5(---) and R_2Co_{17} (...) are shown.

Table 1. Designation of Layers in Rare Earth-Cobalt Intermetallics in Relation to Fig. 4

Key Positions	R-Layer	Mixed Layer	Compact Co-Layer	Dispersed Co-Layer	Phase's
X,Y,Z	α,β,γ	———	$(Co)_A$, $(Co)_B$, $(Co)_C$	a, b, c	RCo_2
X,Y,Z	α,β,γ	x, y, z	$(Co)_A$, $(Co)_B$, $(Co)_C$	a, b, c	RCo_3 R_2Co_7 R_5Co_{17}
X,Y,Z	———	x=y=z	$(Co)_A$=$(Co)_B$=$(Co)_C$=(Co)	———	RCo_5
X_1,X_2,Z_3 Y_1,Y_2,Y_3 Z_1,Z_2,Z_3	———	x_1,x_2,x_3 y_1,y_2,y_3 z_1,z_2,z_3	$(Co)_A$=$(Co)_B$=$(Co)_C$=(Co)	———	R_2Co_{17}

results in the propagation of extensive faulting. The spacial ordering of such faults produces new structures.

Similarly in high ordered phases, transformations involving both structural and compositional changes are often achieved by the growth of "compositional faults", the formation of which also is accompanied normally by a lattice shear. Accordingly the resultant phases are commonly called shear structures; the compositional faults are called CS (crystallographic shear) planes or non-conservative APB (antiphase boundaries). The edgewise boundary of such a CS plane within the parent crystal is a sessile partial dislocation, edgewise growth of the fault corresponding to its climb. The spacial ordering of CS planes produces new structures just as in the case of regular faulting in a shear transformation.

The question of CS planes has been raised in connection with the mechanism of the eutectoid decomposition of $SmCo_5$ (7,8) and now as a way of developing a host of compounds from RCo_2-R_2Co_{17} Both involve systematic substituion of R for Co in some of the mixed layers, which create an unstable geometrical situation

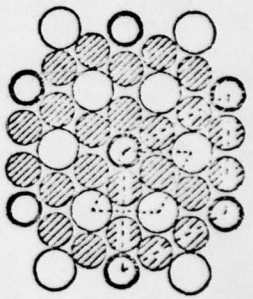

Fig. 5. The mixed atom layer of the Th_2Zn_{17} and Th_2Ni_{17} structures of R_2Co_{17}.

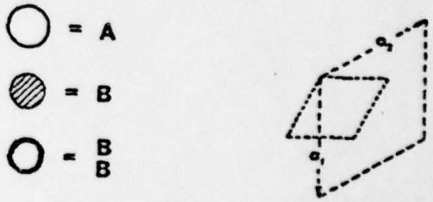

relieved partly by shear. For instance this may be represented in the formation of R_2Co_7 from RCo_5 (4) as

$$3\ RCo_5 - Co + R = R_2Co_{14}.$$

In terms of the stacking sequence notation, a mixed layer, for example z, is modified in the following manner by this substitution:

$$z - Co + R \rightarrow \begin{matrix} Y \\ a \\ \beta \end{matrix} \quad \text{or} \quad \begin{matrix} Y \\ b \\ \alpha \end{matrix}$$

depending on the Co chosen. This is just the central part of the Laves phase AB_2 or of AB_3 or A_2B_7 depicted in Fig. 1. For R_2Co_7, such a reaction must occur every third mixed layer. All of the structures in the composition interval RCo_2 - RCo_5 may be regarded as shear structures based on RCo_5.

Essentially the same thing is true of R_2Co_{17} where diviation from stoichiometry may possibly be accommodated by CS plane formation. The structure is more complicated than in the previous case, however, because of the presence of Co-pairs in the mixed R/Co layers. The essential result is the same though as illustrated by Fig. 6 which shows a CS plane model for RCo_5, (8, corrected) and R_2Co_{17} (9). In the latter case the particular section shown does not include the Co-pairs associated with the planar defect, however. In both cases, sessile partial dislocations, M and N, are also shown, along with lattice displacements characterizing the defects. As determined for $SmCo_5$ (7), the shear displacement vector R produces a systematic shift in the stacking sequence notation for the lower part of the crystal of the type $Z_2 \rightarrow Y_1$, Y_2 or Y_3. That is, if $Z_2 \rightarrow Y_1$, then $z_2 \rightarrow y_1$, $(Co)_B \rightarrow (Co)_A$ etc.

The faulting accompanying shear transformations has been discussed at length for R_2Co_{17} (5,6,10) and is illustrated in Fig. 7 for the case of $2H^2 \rightarrow 4H$. Each dashed line represents the glide plane of a glissile transformation dislocation having one of three Burgers vectors appropriate to the displacement indicated. In like manner it is possible to generate any stacking sequence for phases such as RCo_3, R_2Co_7 etc.

Returning finally to the question of homologous series of phases in the composition interval RCo_2 to RCo_5, Fig. 8 compares the stacking sequence representation to the Cromer-Larson scheme (4) for the unit cell of one of the 1H forms of R_2Co_{17}. Here the Cromer-Larson scheme has been modified slightly to emphasize the location of CS planes within the basic RCo_5 pattern. It should be noted that there are several fundamentally different 1H forms of this phase in addition to that shown in Fig. 8,

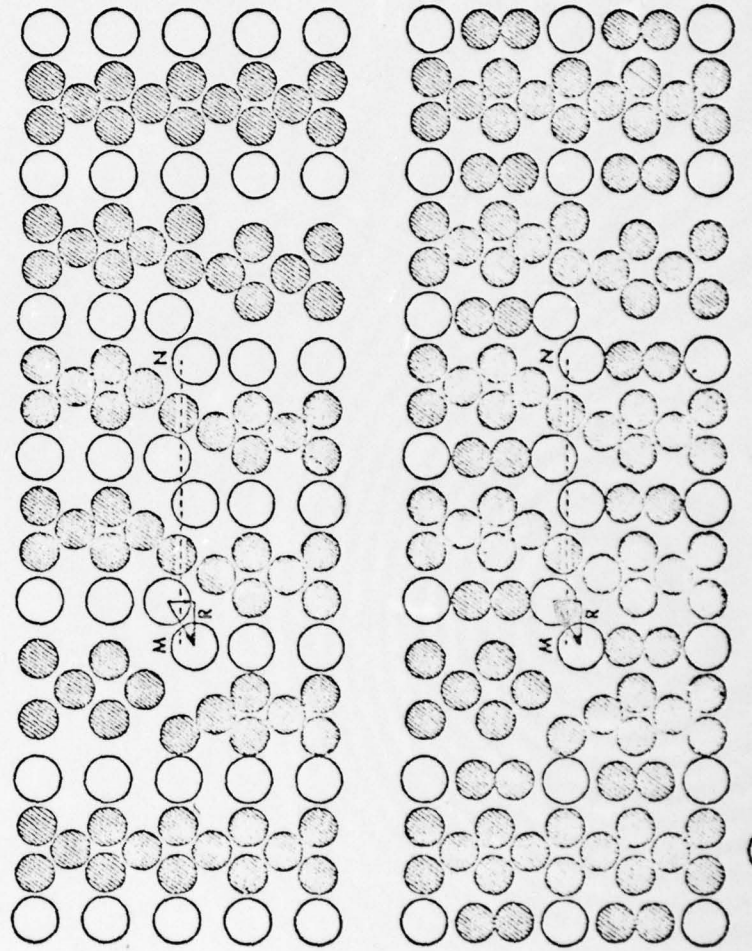

○ = A

Fig. 6. CS planes limited by sessile partial dislocation in RCo_5 (after (8), corrected) and in R_2Co_{17} (after (9)).

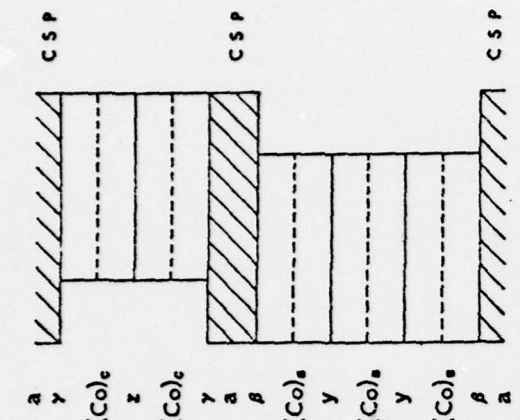

Fig. 8. Comparison of the stacking sequence and Cromer-Larson representations of a 1H form of R_7Co_{23}.

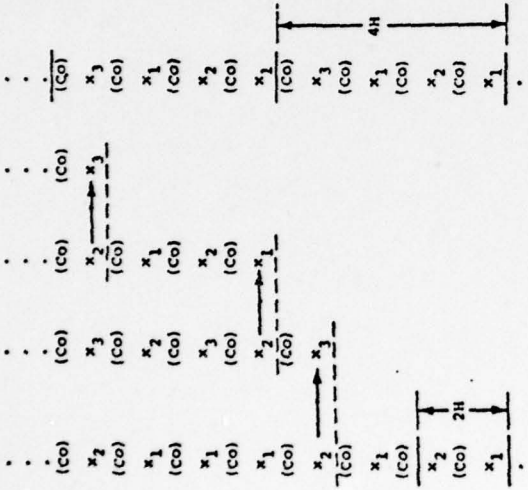

Fig. 7. Imperfect slip model for the transformation 2H → 4H in R_2Co_{17}.

including

$$\ldots a\beta(Co)_B\gamma(Co)_B\beta c\alpha(Co)_A x(Co)_A x(Co)_A \alpha c\beta(Co)_B\gamma(Co)_B\beta a$$
$$\gamma(Co)_C z(Co)_C z(Co)_C \gamma a\ldots$$

and

$$\ldots a\beta(Co)_B\gamma(Co)_B\beta a\gamma(Co)_C z(Co)_C z(Co)_C \gamma b\alpha(Co)_A x(Co)_A \alpha b$$
$$\gamma(Co)_C z(Co)_C z(Co)_C \gamma a\ldots$$

It may be possible to determine the specific local "structural code" for such a phase by high resolution direct lattice resolution electron microscopy, there being a large difference in electron scattering powers of the R- and Co- atoms.

Acknowledgments: Research sponsored by the National Science Foundation (CWA and KCL) and by the Office of Naval Research (AEM).

References:

1. Cromer, D. T., and C. E. Olsen, "The Crystal Structures of $PuNi_3$ and $CeNi_3$," Acta Cryst. 12, 689 (1959).
2. Cromer, D. T., and A. C. Larson, "The Crystal Structure of Ce_2Ni_7," ibid 12, 855-859 (1959).
3. Buschow, K.H. J., "Crystal Structures, Magnetic Properties and Phase Relations of Erbium-Nickel Intermetallic Compounds" J. Less-Comm. Met. 16, 45-53 (1968).
4. Strnat, K. J., and A. E. Ray, "Evidence for New Magnetic Rare Earth-Cobalt Phases," Proc. 3M Conf. 680-682 (1974).
5. Allen, C. W., D. L. Kuruzar and A. E. Miller, "Possible Magnetic Significance of Faults and Polytypes in R_2Co_{17} Compounds," IEEE Trans. MAG-10, No. 3, 716-719 (1974).
6. Allen, C. W., A. E. Miller and D. L. Kuruzar, "Multiple Structures and Faulting in the Intermetallics R_2Co_{17}," 8th Int. Cong. on E. M., Canberra I, 638-639 (1974).
7. Rao, P., J. G. Smeggil and E. F. Koch, "Phase Transformations in Co_5Sm," 31st Ann. Proc. EMSA, Claitor's Publ. Div., Baton Rouge, 186-187 (1973).
8. Smeggil, J. G., P. Rao, J. D. Livingston and E. F. Koch, "Thermal Decomposition and Magnetic Behavior of Co_5Sm," AIP Conf. Proc. No. 18, 1144-1148 (1974).
9. Kuruzar, D. L., "Structures and Defects in Rare-Earth/Transition Element Intermetallics," Masters Thesis, U. of Notre Dame (1975).
10. Allen, C. W., and D. L. Kuruzar, "Generation of 4H and 6H Structures During the Hexagonal-Rhombohedral Transformation in Dy_2Co_{17}", 33rd Ann. Proc. EMSA, Las Vegas, 38-39 (1975).

MAGNETIZATION, MAGNETOCRYSTALLINE ANISOTROPY AND MAGNETOSTRICTION OF Tb_2Co_{17}, Ho_2Co_{17} AND Er_2Co_{17} SINGLE CRYSTALS*

A. E. Miller, T. D'Silva and H. Rodrigues
Department of Metallurgical Engineering and Materials Science
University of Notre Dame, Notre Dame, Indiana 46556

ABSTRACT

This paper describes the temperature dependence of magnetization, the anisotropy constant K_1 and the magnetostriction constant λ^γ of single crystals of Tb_2Co_{17}, Ho_2Co_{17} and Er_2Co_{17} over the temperature range 77.4°K to 400°K. Tb_2Co_{17} and Ho_2Co_{17} have a uniformly easy magnetization in the basal plane while Er_2Co_{17} maintains an easy C axis over the entire temperature range. The anisotropy constant K_1 was determined by a least square fit of the theoretical equation of magnetization to the measured magnetization curve along the hard axis. The anisotropy constant K_1 at 297°K for Tb_2Co_{17}, Ho_2Co_{17} and Er_2Co_{17} is, -3.2×10^7, -0.9×10^7 and 0.41×10^7 ergs/cm^3, respectively.

The magnetostriction coefficient λ^γ was determined by the strain gage technique. The contribution of the Tb ion to the magnetostriction constant λ^γ of the R_2Co_{17} compound is positive whereas the contribution of the Ho ion is negative. The magnetostrictive behavior of the Tb ion is single ion in nature.

INTRODUCTION

The purpose of this paper is to describe a study of the saturation magnetization, magnetocrystalline anisotropy and magnetostrictive behavior of Tb_2Co_{17}, Ho_2Co_{17} and Er_2Co_{17} and to test for the single ion nature of the rare earth ions in these compounds. Similar studies on R_2Co_{17} compounds of other heavy rare earth elements have been reported earlier.[1-5]

The magnetocrystalline anisotropy energy for a hexagonal crystal is given by,[6]

$$E_A = K_1\sin^2\theta + K_2\sin^4\theta \qquad (1)$$

The anisotropy constants K_1 and K_2 can be determined by a least square fit of the theoretical equation of magnetization to the experimentally determined magnetization curve along the hard axis.[7] Since the anisotropy constant K_2 is dependent on the curvature of the magnetization curve, determined along the hard axis, the complete magnetization curve along the hard axis must be available to determine K_2 accurately.

The magnetostrictive strain in hexagonal crystals as a function of the direction cosines of magnetization, direction cosines of strain measurement and the magnetostriction constants is given by Callen and Callen.[8] The magnetostriction constant λ^γ measures the distortion in the basal plane and is determined by selecting the a axis as the strain gage direction and the a and b axes as the initial and final directions of magnetization respectively.

The magnetization $(m)^R$ of the rare earth sublattice R is taken to be given by:

$$m^R = m^{R_2Co_{17}} - m^{Co} \qquad (2)$$

The anisotropy constant K_1^R and the magnetostriction constant $(\lambda^\gamma)^R$ are defined in a similar fashion.

For single ion behavior, the magnetostriction constant $(\lambda^\gamma)^R$ and the anisotropy coefficient k_2 (where $k_2^R = K_1^R + \frac{6}{7}K_2^R$)[9] are related to the magnetization of the rare earth sublattice by a hyperbolic Bessel function[8,10] given below.

$$[\lambda^\gamma(T,H)]^R = [\lambda^\gamma(0,H)]^R\ \hat{I}_{5/2}\{\mathcal{L}^{-1}(\tfrac{m}{m_o})^R\} \qquad (3)$$

$$k_2^R = k_2^R(0)\ I_{5/2}\{\mathcal{L}^{-1}(\tfrac{m}{m_o})^R\} \qquad (4)$$

where, the argument of the Bessel function is the inverse Langevin function of the reduced magnetization of the rare earth sublattice. The single ion nature of the rare earth ion in compounds with transition metals and in pure elements, is reported in literature.[11,12]

EXPERIMENTAL

The saturation magnetization, magnetization curves in the easy and hard directions, and the magnetostriction constant λ^γ were determined from 77.4°K to 400°K on single crystals of the three compounds. Details of specimen preparation and experimental technique are described in previous papers.[1-4]

RESULTS AND DISCUSSION

Tb_2Co_{17} and Ho_2Co_{17} are both easy basal plane and Er_2Co_{17} is easy C axis. The field dependence of the magnetization along easy and hard directions for Tb_2Co_{17}, Ho_2Co_{17} and Er_2Co_{17} are shown in Figs. 1, 2, and 3, respectively. Fig. 4 shows the temperature dependence of the saturation magnetization determined from the magnetization curves in the easy direction. The saturation magnetization measured on aligned powders[13,14,15] of these compounds and single crystals[16] of Tb_2Co_{17} and Ho_2Co_{17}, was determined by the extrapolation technique. The M_S value of Tb_2Co_{17} only, agrees with that reported by Strnat et al.[14] The saturation magnetization of the R-Co compounds depends on the composition, which is controlled by the purity of the starting materials and the alloy preparation technique. The crystals used in this study were all Co rich with chemically analysed compositions of $Tb_2Co_{17.05}$, $Er_2Co_{17.03}$ and $Ho_2Co_{17.46}$. This could explain the higher M_S values for Tb_2Co_{17} and Ho_2Co_{17} in comparison to those reported by Deryagin and Kudrevatykh.[16]

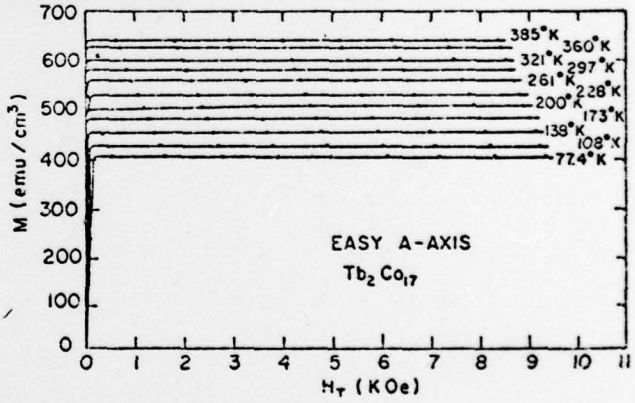

Fig. 1(a). The true field dependence of magnetization along the easy a axis for Tb_2Co_{17}

Fig. 5 shows the temperature dependence of K_1 for Er_2Co_{17}, Ho_2Co_{17} and Tb_2Co_{17}. The K_1 values for these compounds were determined from the initial segment of the magnetization curves in the hard direction. The K_1 values for Tb_2Co_{17} and Ho_2Co_{17} agree fairly well with the K_{eff} values reported by Deryagin and Kudrevatykh.[16] The anisotropy constant K_1 of Er_2Co_{17} at 297°K measured on aligned powder by Narasimhan et al,[15] is 0.27×10^7ergs/cc as compared to 0.4×10^7ergs/cc reported in this study.

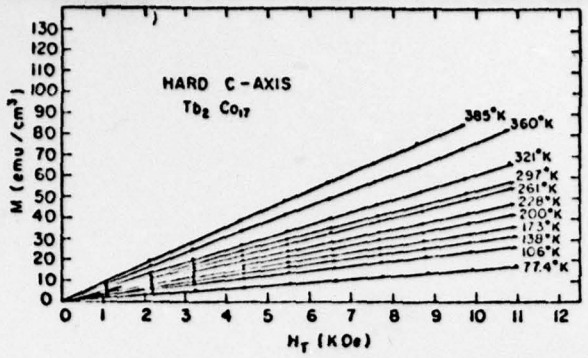

Fig. 1(b). The true field dependence of magnetization along the hard c axis for Tb_2Co_{17}.

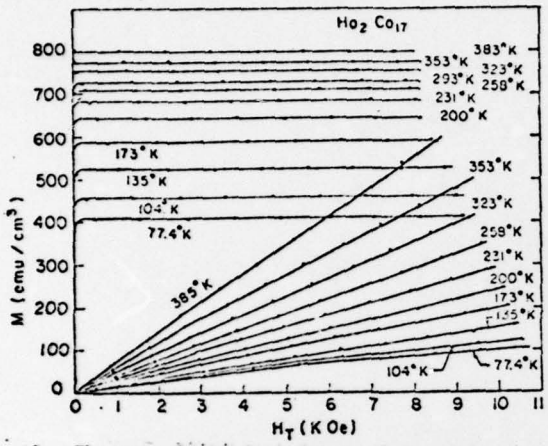

Fig. 2. The true field dependence of magnetization along the easy a axis and the hard c axis for Ho_2Co_{17}.

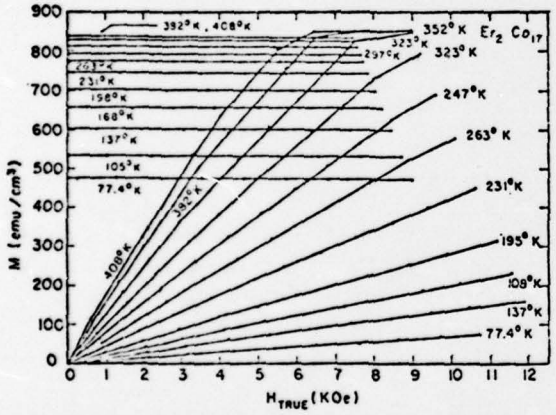

Fig. 3. The true field dependence of magnetization along the easy c axis and hard a axis for Er_2Co_{17}.

Fig. 6 shows the temperature dependence of the magnetostriction constant $\lambda\gamma$ for Tb_2Co_{17} and Ho_2Co_{17}. The constant $\lambda\gamma$ for Er_2Co_{17} could not be determined because of lack of saturation in the basal plane, with available fields. The Tb ion has a positive contribution to the magnetostriction of the R_2Co_{17} compounds whereas the contribution of the Ho ion is negative. This is due to the difference in shape between the two rare earth ions.[17]

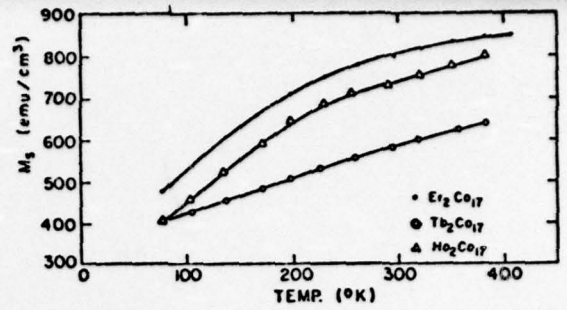

Fig. 4. The temperature dependence of saturation magnetization.

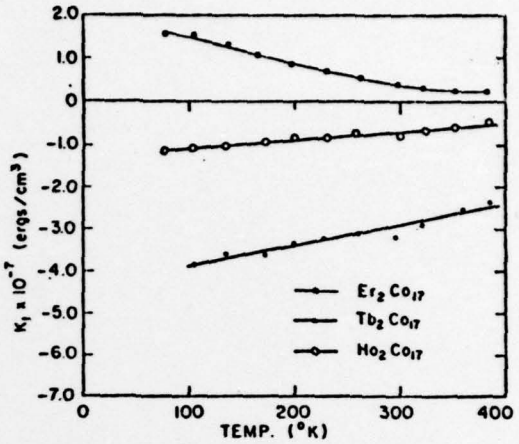

Fig. 5. The temperature dependence of the anisotropy constant K_1 for Tb_2Co_{17} Er_2Co_{17} and Ho_2Co_{17}.

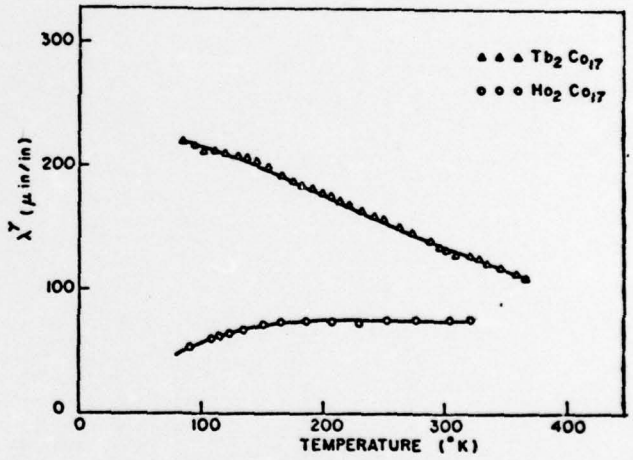

Fig. 6. The temperature dependence of λ^Y for Tb_2Co_{17} and Ho_2Co_{17}.

The cobalt contribution to the Tb_2Co_{17} and Ho_2Co_{17} is determined from Y_2Co_{17} which is also easy basal plane. Although pure Co differs structurally, the K_1 values for pure Co reported in literature,[18] is used for determining the Co contribution to K_1 for Er_2Co_{17}, since pure Co and the Co sublattice in Er_2Co_{17} both have an easy C-axis and therefore the same sign for K_1. Since the anisotropy constant K_2 could not be determined accurately, the anisotropy constant K_1 is used in Equation 4 which is plotted in Figs. 7,8 and 9 for Tb_2Co_{17}, Ho_2Co_{17} and Er_2Co_{17}, respectively. Only the Er ion shows good agreement with

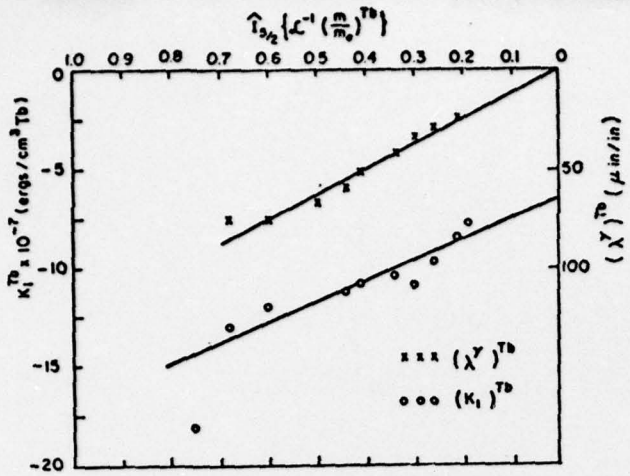

Fig. 7. The magnetization dependence of K_1^{Tb} and $(\lambda^\gamma)^{Tb}$ for the Tb ion.

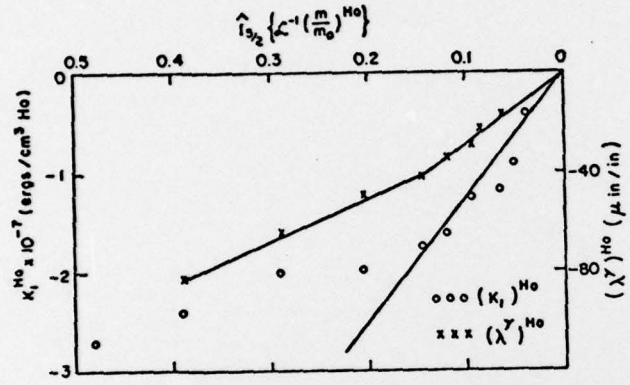

Fig. 8. The magnetization dependence of K_1^{Ho} and $(\lambda^\gamma)^{Ho}$ for the Ho ion.

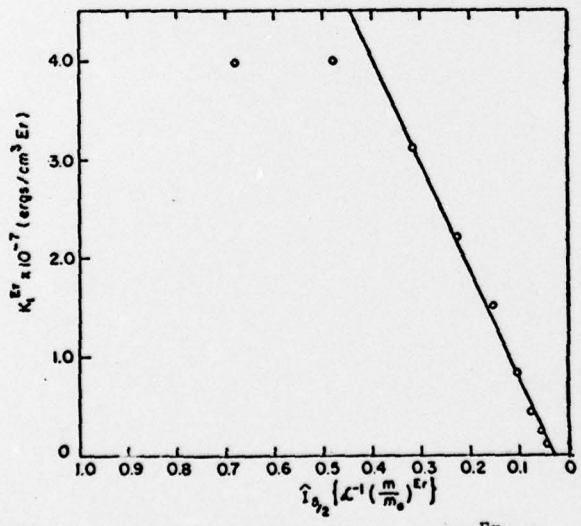

Fig. 9. The magnetization dependence of K_1^{Er} for the Er ion.

single ion anisotropy behavior which may indicate that K_2^R is not as significant in Er_2Co_{17} as in the other compounds. The contribution to magnetostriction of the Tb and Ho ions are showsn in Figs. 9 and 10. The magnetostriction of the Tb ion shows excellent agreement with single ion behavior whereas the deviation of the Ho ion from this behavior is not understood.

**Work supported by the Office of Naval Research.

REFERENCES

1. D'Silva T., Igarashi H., Miller A.E., Magnetization and Magnetostriction in Y_2Co_{17} and Dy_2Co_{17}, Proceedings of the 10th Rare Earth Research Conf., 1, 458-465, (1973).
2. Miller A.E., D'Silva T., Igarashi H., Shanley J., Magnetostriction of Dy_2Co_{17}, Y_2Co_{17} and $Dy_xY_{2-x}Co_{17}$ Intermetallics, AIP Conference Proceedings, 18, 1253-1255, (1973).
3. Miller A.E., D'Silva T., Miura K., Magnetization and Magnetostriction in Lu_2Co_{17}, Tm_2Co_{17} and $Lu_xTm_{2-x}Co_{17}$ Intermetallics, Proceedings of the 11th Rare Earth Research Conf., 1, 461-468, (1974).
4. Miller A.E., Shanley J.F., D'Silva T., Magnetization and Magnetic Anisotropy in $Y_xDy_{2-x}Co_{17}$ Intermetallics, Proceedings of the 11th Rare Earth Research Conf., 1, 469-472, (1974).
5. Miller A.E., Miura K., Rodrigues H., D'Silva T., Magnetization and Magnetic Anisotropy in $Lu_xTm_{2-x}Co_{17}$ Intermetallics, AIP Conference Proceedings, 24, 672-673, (1974).
6. Mason W.P., Derivation of Magnetostriction and Anisotropy Energies for Hexagonal, Tetragonal and Orthorhombic Crystals, Physical Review, 96, 302-305, (1954).
7. Sucksmith W., Thompson J.E., The magnetic anisotrophy of cobalt, Proceedings of the Royal Society, 362-375, (1954).
8. Callen E., Callen H., Magnetostriction, Forced Magnetostriction and Anomalous Thermal Expansion in Ferromagnets, Physical Review, 139, A455-A471, (1965).
9. Kneller E., Ferromagnetismus, Springer Verlag, Berlin, (1962).
10. Callen H., Shtrikman S., A Probability density common to molecular field and collective excitation theories of Ferromagnetism, Solid State Comm., 3, 5-8, (1965).
11. Clark A.E., Magnetic and Magnetoelastic properties of highly magnetostrictive rare earth-iron Laves phase compound, AIP Conference Proceedings, 18, 1015-1029, (1973).
12. Clark A.E., DeSavage B.F., Bozorth R., Anomalous Thermal Expansion and magnetostriction of Single Crystal Dysprosium, Physical Review, 138, A216-A224, (1965).
13. LaForest J., Lemaire R., Pauthenet R., Schweiger J., Propriétés magnétostatiques des alliages T_2Co_{17} dans lesquels T est un métal des terres rares ou l'yttrium, C. R. Acad. Sc. Paris, 262, 1260-1263, (1966).
14. Strnat K., Hoffer G., Ostertag W., Olson J.C., Ferrimagnetism of the Rare Earth-Cobalt Intermetallic Compound, R_2Co_{17}, J. Appl. Phys., 1252-1253, (1966).
15. Narasimhan, K.S.V.L., Wallace W.E., Hutchens R.D., Greedan J.E., Magnetic Anisotropy of R_2Co_{17} Compounds, AIP Conference Proceedings, 18, 1212-1216, (1973).
16. Steven K.W.H., Matrix Elements and Operator Equivalents Connected with the Magnetic Properties of Rare Earth Ions, Physical Society, 65, 209-215, (1952).
17. Deryagin A.V. and Kudrevatykh N.V., Magnetic Anisotropy of Single Crystals of Intermetallic R_2Co_{17} (R=Tb,Dy,Ho,Lu) Compounds, Phys. Stat. Solidi, (a) 30, K129, (1975).
18. Barnier Y., Pauthenet R., Rimet G., Thermomagnetic Study of a Hexagonal Cobalt Single Crystal, Cobalt, 15, 1-7, (1962).

BASIC DISTRIBUTION LIST

Address	No. of Copies
Office of Naval Research Code 471 Department of the Navy Arlington, Virginia 22217	3
Office of Naval Research Code 105 Department of the Navy Arlington, Virginia 22217	6
Office of Naval Research Code 474 Department of the Navy Arlington, Virginia 22217	1
Director Office of Naval Research Branch Office 495 Summer Street Boston, Massachusetts 02210	1
Office of Naval Research New York Area Office 207 West 24th Street New York, New York 10011	1
Director Office of Naval Research Branch Office 536 South Clark Street Chicago, Illinois 60605	1
Director Office of Naval Research Branch Office 1030 East Green Street Pasadena, California 91106	1
Office of Naval Research San Francisco Area Office 760 Market Street, Room 447 San Francisco, California 94102	1
Commanding Officer Naval Weapons Laboratory Dahlgren, Virginia 22448	
Attn: Research Division	1

Address	No. of Copies
Director Code 2000 Naval Research Laboratory Washington, D. C. 20390	
Attn: Technical Information Officer	1
Director Code 2020 Naval Research Laboratory Washington, D.C. 20390	
Attn: Technical Information Officer	1
Director Code 6000 Naval Research Laboratory Washington, D.C. 20390	
Attn: Technical Information Officer	1
Director Code 6100 Naval Research Laboratory Washington, D.C. 20390	
Attn: Technical Information Officer	1
Director Code 6300 Naval Research Laboratory Washington, D.C. 20390	
Attn: Technical Information Officer	1
Director Code 6400 Naval Research Laboratory Washington, D.C. 20390	
Attn: Technical Information Officer	1
Director Code 2627 Naval Research Laboratory Washington, D.C. 20390	
Attn: Technical Information Officer	6
Commander Code 320A Naval Air Systems Command Department of the Navy Washington, D.C. 20360	1

Address	No. of Copies
Commander Code 5203 Naval Air Systems Command Department of the Navy Washington, D.C. 20360	1
Commander Code ORD 033 Naval Ordnance Systems Command Department of the Navy Washington, D.C. 20360	1
Mr. F. S. Williams Naval Air Development Center Code 302 Warminster, Pennsylvania 18974	1
Commanding Officer Code 210 Naval Ordnance Laboratory White Oak Silver Spring, Maryland 20910	1
Commander Code 0342 Naval Ship Systems Command Department of the Navy Washington, D.C. 20360	1
Commanding Officer Code L70 Naval Civil Engineering Laboratory Port Hueneme, California 93041	1
Commander Code 6101 Naval Ship Engineering Center Department of the Navy Washington, D.C. 20360	1
Naval Ship R&D Center Code 28 Materials Division Annapolis, Maryland 21402	1
U.S. Naval Postgraduate School Materials Sciences Division Monterey, California 93940	1
Commander Code 5560 Naval Weapons Center China Lake, California 93555	1

Address	No. of Copies
Scientific Advisor Code AX Commandant of the Marine Corps Washington, D.C. 20380	1
Commanding Officer Metallurgy & Ceramics Division Army Research Office Box CM, Duke Station Durham, North Carolina 27706	1
Office of Scientific Research Solid State Division (SRPS) Department of the Air Force Washington, D.C. 20333	1
Defense Documentation Center Cameron Station Alexandria, Virginia 22314	12
National Bureau of Standards Metallurgy Division Washington, D.C. 20234	1
National Bureau of Standards Inorganic Materials Division Washington, D.C. 20234	1
Atomic Energy Commission Metals & Materials Branch Washington, D.C. 20545	1
Argonne National Laboratory Metallurgy Division P.O. Box 299 Lemont, Illinois 60439	1
Brookhaven National Laboratory Technical Information Division Upton, Long Island, N.Y. 11973	
Attn: Research Library	1
Director Metals and Ceramics Division Oak Ridge National Laboratory P.O. Box X Oak Ridge, Tennessee 37830	1

Address	No. of Copies
Los Alamos Scientific Laboratory Report Librarian P.O. Box 1663 Los Alamos, New Mexico 87544	1
Commanding Officer Army Materials and Mechanics Research Center Watertown, Massachusetts 02172	
Attn: Res. Programs Office (AMXMR-P)	1
Library Bldg. 50, Room 134 Lawrence Radiation Laboratory Berkeley, California 94720	1
Commanding Officer Naval Underwater Systems Center Newport, Rhode Island 02840	1
Aerospace Research Laboratories Wright-Patterson AFB Building 450 Dayton, Ohio 45433	1
Defense Metals Information Center Battelle Memorial Institute 505 King Avenue Columbus, Ohio 43201	1
Defense Ceramics Information Center Battelle Memorial Institute 505 King Avenue Columbus, Ohio 43201	1
Army Electronics Command Evans Signal Laboratory Solid State Devices Branch c/o Senior Navy Liaison Officer Fort Monmouth, New Jersey 07703	1
Commanding General Department of the Army Frankford Arsenal Philadelphia, Pennsylvania 19137	
Attn: ORDBA-1320, 64-4	1
Executive Director Materials Advisory Board National Academy of Sciences 2101 Constitution Avenue, N.W. Washington, D.C. 20418	1

Address	No. of Copies
NASA Headquarters Code RRM Washington, D.C. 20546	1
AFML/MX Wright-Patterson AFB, Ohio 45433	1
Advanced Research Projects Agency 1400 Wilson Boulevard Arlington, Virginia 22209	
Attn: Director, Materials Sciences	1
HQDA (DARD-ARS-P/Dr. J. Bryant) Washington, D.C. 20310	1
Department of Interior Science and Engineering Advisor Bureau of Mines Washington, D.C. 20240	1
National Aeronautics & Space Adm. Librarian Lewis Research Center 21000 Brookpark Road Cleveland, Ohio 44135	1
Naval Missile Center Materials Consultant Code 3312-1 Point Mugu, California 93041	1
Commanding Officer Naval Weapons Center Corona Labs. Corona, California 91720	1
Commander Naval Air Test Center Weapons Systems Test Division Code 01A Patuxent River, Maryland 20670	1
Director Ordnance Research Laboratory P.O. Box 30 State College, Pennsylvania 16801	1
Commander Naval Undersea Warfare Center 271 Catalina Boulevard San Diego, California 92152	1

Address	No. of Copies
Director Applied Physics Laboratory Johns Hopkins University 8621 Georgia Avenue Silver Spring, Maryland 20901	1
Director Applied Physics Laboratory University of Washington 1013 Northeast Fortieth Street Seattle, Washington 98105	1
Materials Sciences Group Code S130.1 Navy Electronics Laboratory 271 Catalina Boulevard San Diego, California 92152	1
Commanding Officer Naval Ships R&D Center Washington, D.C. 20007	
Attn: Code 747	1
Materials Sciences Corporation Blue Bell Office Campus 1777 Walton Road Blue Bell, Pennsylvania 19422	1
Mr. Richard J. Janowiecki Monsanto Research Corporation Dayton Laboratory 1515 Nicholas Road Dayton, Ohio 45407	1

SUPPLEMENTARY DISTRIBUTION LIST

Address

Professor G. S. Ansell
Rensselaer Polytechnic Institute
Dept. of Metallurgical Engineering
Troy, New York 12181

Professor H. D. Brody
University of Pittsburgh
School of Engineering
Pittsburgh, Pennsylvania 15213

Professor J. B. Cohen
Northwestern University
Dept. of Material Sciences
Evanston, Illinois 60201

Professor M. Cohen
Massachusetts Institute of
Technology
Department of Metallurgy
Cambridge, Massachusetts 02100

Professor B. C. Giessen
Northeastern University
Department of Chemistry
Boston, Massachusetts 02115

Dr. G. T. Hahn
Battelle Memorial Institute
Department of Metallurgy
505 King Avenue
Columbus, Ohio 43201

Professor R. W. Heckel
Carnegie-Mellon University
Schenley Park
Pittsburgh, Pennsylvania 15213

Professor R. F. Hehemann
Case Western Reserve University
Dept. of Metallurgy & Matls. Sci.
Cleveland, Ohio 44106

Professor G. Judd
Rensselaer Polytech Institute
Dept. of Materials Engineering
Troy, New York 12181

Professor A. Lawley
Drexel University
Dept. of Metallurgical Engr.
Philadelphia, Pennsylvania 19104

Address

Professor R. Maddin
University of Pennsylvania
School of Metallurgical Engr.
Philadelphia, Pennsylvania 19105

Professor J. W. Morris, Jr.
University of California
College of Engineering
Berkeley, California 94720

Professor R. M. Rose
Massachusetts Institute of
Technology
Department of Metallurgy
Cambridge, Massachusetts 02100

Professor O. D. Sherby
Stanford University
Materials Sciences Department
Stanford, California 94300

Professor J. Shyne
Stanford University
Materials Sciences Department
Stanford, California 94300

Professor N. S. Stoloff
Rensselaer Polytechnic Institute
School of Engineering
Troy, New York 12181

Dr. E. R. Thompson
United Aircraft Res. Laboratories
400 Main Street
East Hartford, Connecticut 06108

Professor David Turnbull
Harvard University
Division of Engineering and
Applied Physics
Cambridge, Massachusetts 02100

Professor H. G. F. Wilsdorf
University of Virginia
Department of Materials Science
Charlottesville, Virginia 22903

Dr. J. C. Williams
Rockwell International
Science Center
P.O. Box 1085
Thousand Oaks, California 91360

Dr. C. S. Kortovich
TRW, Inc.
23555 Euclid Avenue
Cleveland, Ohio 44117

Address

Professor D. A. Koss
Michigan Technological University
College of Engineering
Houghton, Michigan 49931

Dr. E. A. Starke, Jr.
Georgia Institute of Technology
School of Chemical Engineering
Atlanta, Georgia 30332

Dr. W. A. Spitzig
U.S. Steel Corporation
Research Laboratory
Monroeville, Pennsylvania 15146

Dr. M. A. Wright
University of Tennessee
Space Institute
Department of Metallurgical Engr.
Tullahoma, Tennessee 37388

Dr. L. Leonard
The Franklin Institute Research Labs
The Benjamin Franklin Parkway
Philadelphia, Pennsylvania 19103

Professor L. E. Murr
New Mexico Institute of
Mining and Tech.
Metallurgical Engineering
Socorro, New Mexico 87801

Dr. G. H. Meier
University of Pittsburgh
Dept. of Metallurgical and
Materials Engineering
Pittsburgh, Pennsylvania 15213

Dr. J. R. Low, Jr.
Carnegie-Mellon University
Metals Research Laboratory
Schenley Park
Pittsburgh, Pennsylvania 15213

Professor H. K. Birnbaum
University of Illinois
Department of Metallurgy
Urbana, Illinois 61801

Dr. F. E. Wang
Naval Ordnance Laboratory
Physics Laboratory
White Oak
Silver Spring, Maryland 20910